Tenth-Order QED Contribution to the Electron $g-2$ and an Improved Value of the Fine Structure Constant

Tatsumi Aoyama,[1,2] Masashi Hayakawa,[3,2] Toichiro Kinoshita,[4,2] and Makiko Nio[2]

[1] Kobayashi-Maskawa Institute for the Origin of Particles and the Universe (KMI), Nagoya University, Nagoya, 464-8602, Japan
[2] Nishina Center, RIKEN, Wako, Japan 351-0198
[3] Department of Physics, Nagoya University, Nagoya, Japan 464-8602
[4] Laboratory for Elementary Particle Physics, Cornell University, Ithaca, New York, 14853, U.S.A
(Dated: August 21, 2012)

This paper presents the complete QED contribution to the electron $g-2$ up to the tenth order. With the help of the automatic code generator, we have evaluated all 12672 diagrams of the tenth-order diagrams and obtained $9.16\,(58)(\alpha/\pi)^5$. We have also improved the eighth-order contribution obtaining $-1.9097\,(20)(\alpha/\pi)^4$, which includes the mass-dependent contributions. These results lead to $a_e(\text{theory}) = 1\,159\,652\,181.78\,(77) \times 10^{-12}$. The improved value of the fine-structure constant $\alpha^{-1} = 137.035\,999\,174\,(35)\,[0.25\text{ppb}]$ is also derived from the theory and measurement of a_e.

PACS numbers: 13.40.Em, 14.60.Cd, 06.20.Jr, 12.20.Ds

The anomalous magnetic moment $a_e \equiv (g-2)/2$ of the electron has played the central role in testing the validity of quantum electrodynamics (QED) as well as the standard model of the elementary particles. On the experimental side the measurement of a_e by the Harvard group has reached the astonishing precision [1, 2]:

$$a_e(\text{HV}) = 1\,159\,652\,180.73\,(0.28) \times 10^{-12}\,[0.24\text{ppb}] \quad (1)$$

In the standard model the contribution to a_e comes from three types of interactions, electromagnetic, hadronic, and electroweak:

$$a_e = a_e(\text{QED}) + a_e(\text{hadronic}) + a_e(\text{electroweak}). \quad (2)$$

The QED contribution can be evaluated by the perturbative expansion in α/π:

$$a_e(\text{QED}) = \sum_{n=1}^{\infty} \left(\frac{\alpha}{\pi}\right)^n a_e^{(2n)}, \quad (3)$$

where $a_e^{(2n)}$ is finite due to the renormalizability of QED and may be written in general as

$$a_e^{(2n)} = A_1^{(2n)} + A_2^{(2n)}(m_e/m_\mu) + A_2^{(2n)}(m_e/m_\tau) + A_3^{(2n)}(m_e/m_\mu, m_e/m_\tau) \quad (4)$$

to show the mass-dependence explicitly. We use the latest values of the electron-muon mass ratio $m_e/m_\mu = 4.836\,331\,66\,(12) \times 10^{-3}$ and the electron-tau mass ratio $m_e/m_\tau = 2.875\,92\,(26) \times 10^{-4}$ [3].

The first three terms of $A_1^{(2n)}$ are known analytically [4–7], while $A_1^{(8)}$ and $A_1^{(10)}$ are known only by numerical integration [8, 9]. They are summarized as:

$$A_1^{(2)} = 0.5,$$
$$A_1^{(4)} = -0.328\,478\,965\,579\,193\,\ldots,$$
$$A_1^{(6)} = 1.181\,241\,456\,\ldots,$$
$$A_1^{(8)} = -1.9106\,(20), \quad (5)$$
$$A_1^{(10)} = 9.16\,(58). \quad (6)$$

The $A_1^{(8)}$ is obtained from 891 Feynman diagrams classified into 13 gauge-invariant subsets (see Fig. 1). The value $A_1^{(8)} = -1.9144\,(35)$ in [9] was confirmed by the new calculation and replaced by the updated value (5).

The $A_1^{(10)}$ receives the contribution from 12672 diagrams classified into 32 gauge-invariant subsets (see Fig. 2). The results of 31 gauge-invariant subsets have been published[10–19]. The remaining set, Set V, consists of 6354 diagrams, which are more than half of all tenth-order diagrams. However, we have managed to evaluate it [20] with a precision which leads to theory more accurate than that of the measurement (1):

$$A_1^{(10)}[\text{Set V}] = 10.092\,(570). \quad (7)$$

Adding data of all 32 gauge-invariant subsets, we are now able to obtain the complete value of $A_1^{(10)}$ as in (6), which replaces the crude estimate $A_1^{(10)} = 0.0(4.6)$ [3, 21, 22].

The mass-dependent terms A_2 and A_3 of the fourth and sixth orders are known [23–28] and re-evaluated using the updated mass ratios [3],

$$A_2^{(4)}(m_e/m_\mu) = 5.197\,386\,67\,(26)\,\times 10^{-7},$$
$$A_2^{(4)}(m_e/m_\tau) = 1.837\,98\,(34)\,\times 10^{-9},$$
$$A_2^{(6)}(m_e/m_\mu) = -7.373\,941\,55\,(27)\,\times 10^{-6},$$
$$A_2^{(6)}(m_e/m_\tau) = -6.583\,0\,(11)\,\times 10^{-8},$$
$$A_3^{(6)}(m_e/m_\mu, m_e/m_\tau) = 0.1909\,(1)\,\times 10^{-12}. \quad (8)$$

Except for $A_3^{(6)}$ all are known analytically so that the uncertainties come only from fermion-mass ratios.

The mass-dependent terms of the eighth order and the muon contribution to the tenth order are numerically evaluated [11–19]. Our new results are summarized as

$$A_2^{(8)}(m_e/m_\mu) = 9.222\ (66)\ \times 10^{-4},$$
$$A_2^{(8)}(m_e/m_\tau) = 8.24\ (12)\ \times 10^{-6},$$
$$A_3^{(8)}(m_e/m_\mu, m_e/m_\tau) = 7.465\ (18)\ \times 10^{-7},$$
$$A_2^{(10)}(m_e/m_\mu) = -0.003\ 82\ (39). \tag{9}$$

The hadronic contribution to a_e is summarized in Ref. [3]. The leading order [29] and next-to-leading order (NLO) [30] contributions of the hadronic vacuum-polarization (v.p.) as well as the hadronic light-by-light-scattering (l-l) term [31] are given as

$$a_e(\text{had. v.p.}) = 1.875\ (18)\ \times 10^{-12},$$
$$a_e(\text{NLO had. v.p.}) = -0.225\ (5)\ \times 10^{-12},$$
$$a_e(\text{had. } l\text{-}l) = 0.035\ (10)\ \times 10^{-12}. \tag{10}$$

At present no direct evaluation of the two-loop electroweak effect is available. The best estimate is the one obtained by scaling down from the electroweak effect on a_μ [32–35]:

$$a_e(\text{weak}) = 0.0297\ (5)\ \times 10^{-12}. \tag{11}$$

To compare the theoretical prediction with the measurement (1), we need the value of the fine-structure constant α determined by a method independent of $g-2$. The best α available at present is the one obtained from the measurement of h/m_{Rb} [36], combined with the very precisely known Rydberg constant and m_{Rb}/m_e [3] :

$$\alpha^{-1}(\text{Rb10}) = 137.035\ 999\ 049\ (90)\quad [0.66\text{ppb}]. \tag{12}$$

With this α the theoretical prediction of a_e becomes

$$a_e(\text{theory}) = 1\ 159\ 652\ 181.78\ (6)(4)(3)(77)$$
$$\times 10^{-12}\quad [0.67\text{ppb}], \tag{13}$$

where the first, second, third, and fourth uncertainties come from the eighth-order term (5), the tenth-order term (6), the hadronic corrections (10), and the fine-structure constant (12), respectively. This is in good agreement with the experiment (1):

$$a_e(\text{HV}) - a_e(\text{theory}) = -1.06\ (0.82) \times 10^{-12}. \tag{14}$$

More rigorous comparision between experiment and theory is hindered by the uncertainty of $\alpha^{-1}(\text{Rb})$ in (12). Note that the sum $1.685(21) \times 10^{-12}$ of the hadronic contributions (10) is now larger than Eq. (14). It is thus desirable to reexamine and update the values of the hadronic contributions.
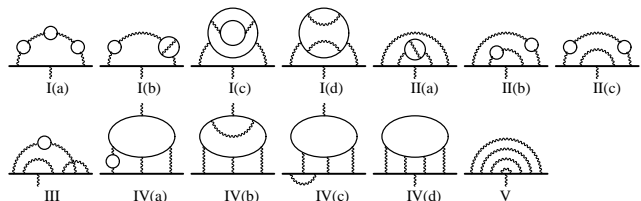

FIG. 1. Typical vertex diagrams representing 13 gauge-invariant subsets contributing to the eighth-order lepton $g-2$.

The equation (13) shows clearly that the largest source of uncertainty is the fine-structure constant (12). To put it differently, it means that a non-QED α, even the best one available at present, is too crude to test QED to the extent achieved by the theory and measurement of a_e. Thus it makes more sense to test QED by an alternative approach, namely, compare $\alpha^{-1}(\text{Rb10})$ with α^{-1} obtained from theory and measurement of a_e. This leads to

$$\alpha^{-1}(a_e) = 137.035\ 999\ 1736\ (68)(46)(26)(331)\quad [0.25\text{ppb}], \tag{15}$$

where the first, second, third, and fourth uncertainties come from the eighth-order and the tenth-order QED terms, the hadronic and electroweak terms, and the measurement of $a_e(\text{HV})$ in (1), respectively. The uncertainty due to theory has been improved by a factor 4.5 compared with the previous one [22].

Let us now discuss the eighth- and tenth-order calculations in more details. The 13 gauge-invariant groups of the eighth order were numerically evaluated by VEGAS [39] and published [9, 10]. As an independent check, we built all programs of the 12 groups from scratch with the help of automatic code generator GENCODEN, except for Group IV(d) which had already been calculated by two different methods [38]. The new values of the mass-independent contributions of all 12 groups are consistent with the old values. We have thus statistically combined two values and listed the results in Table I. Since the validity of the new programs were confirmed in this way, we used the new programs as well as the old programs to evaluate the mass-dependent terms $A_2^{(8)}$ and $A_3^{(8)}$.

Group V deserves a particular attention which consists of 518 vertex diagrams and is the source of the largest uncertainty of $a_e^{(8)}$. The programs generated by GENCODEN have been evaluated with intense numerical work which led to $-2.173\ 77\ (235)$. This is consistent with the value in [9], $-2.179\ 16\ (343)$. The combined value is

$$A_1^{(8)}[\text{Group V}] = -2.175\ 50\ (194)\ . \tag{16}$$

This improvement results in about 40% reduction of the uncertainty of the eighth-order term.

The tenth-order contribution comes from 32 gauge-invariant subsets (see Fig. 2). The FORTRAN programs of integrals of 15 subsets I(a-f), II(a,b), II(f), VI(a-c), VI(e,f), and VI(i) are straightforward and obtained by a

TABLE I. The eighth-order QED contribution from 13 gauge-invariant groups to electron $g-2$. The values with a superscript a, b, or c are quoted from Refs.[37], [8], or [38], respectively. n_f shows the number of vertex diagrams contributing to $A_1^{(8)}$. Other values are obtained from evaluation of new programs. The mass-dependence of $A_3^{(8)}$ is $A_3^{(8)}(m_e/m_\mu, m_e/m_\tau)$.

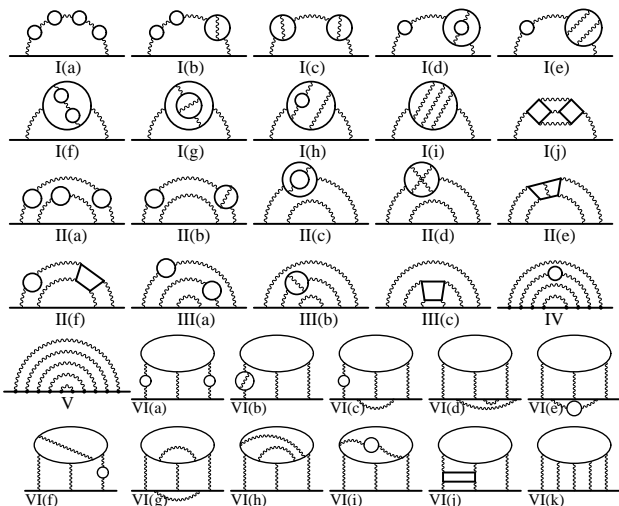| group	n_f	$A_1^{(8)}$	$A_2^{(8)}(m_e/m_\mu) \times 10^3$	$A_2^{(8)}(m_e/m_\tau) \times 10^5$	$A_3^{(8)} \times 10^7$
I(a)	1	0.000 876 865 $\cdots^a$	0.000 226 456 (14)	0.000 080 233 (5)	0.000 011 994 (1)
I(b)	6	0.015 325 20 (37)	0.001 704 139 (76)	0.000 602 805 (26)	0.000 014 097 (1)
I(c)	3	0.011 130 8 (9)^b	0.011 007 2 (15)	0.006 981 9 (12)	0.172 860 (21)
I(d)	15	0.049 514 8 (38)	0.002 472 5 (7)	0.087 44 (1)	0
II(a)	36	-0.420 476 (11)	-0.086 446 (9)	-0.045 648 (7)	0
II(b)	6	-0.027 674 89 (74)	-0.039 000 3 (27)	-0.030 393 7 (42)	-0.458 968 (17)
II(c)	12	-0.073 445 8 (54)	-0.095 097 (24)	-0.071 697 (25)	-1.189 69 (67)
III	150	1.417 637 (67)	0.817 92 (95)	0.6061 (12)	0
IV(a)	18	0.598 838 (19)	0.635 83 (44)	0.451 17 (69)	8.941 (17)
IV(b)	60	0.822 36 (13)	0.041 05 (93)	0.014 31 (95)	0
IV(c)	48	-1.138 52 (20)	-0.1897 (64)	-0.102 (11)	0
IV(d)	18	-0.990 72 (10)^c	-0.1778 (12)	-0.0927 (13)	0
V	518	-2.1755 (20)	0	0	0

FIG. 2. Typical self-energy-like diagrams representing 32 gauge-invariant subsets contributing to the tenth-order lepton $g-2$. Solid lines represent lepton lines propagating in a weak magnetic field.

slight modification of programs for the eighth-order diagrams. Together with the results of subsets VI(j,k), the contributions from 17 subsets to $A_1^{(10)}$ were evaluated and published [10]. We recalculated all 17 subsets once more from scratch and found that the results of I(d), I(f), II(a), II(b), and VI(c) in [10] were incorrect. Although the constructed integrals for the first four subsets are free from errors, they did not include the finite renormalization terms in the last step of the calculation. The value of the subset VI(c) was a typo. The corrected values are listed in Table II.

Other subsets are far more difficult to handle. Thus we developed and utilized the code-generating algorithm GENCODEN which carries out all steps automatically, including subtraction of ultraviolet and infrared divergences [40]. By GENCODEN and its modifications for handling vacuum-polarization loops and light-by-light-scattering loops, we have obtained FORTRAN programs for 12 more subsets [12, 14–18]. The subsets III(c) and I(j), which involve one(two) light-by-light scattering subdiagram(s) internally, were handled manually [11, 19]. The subset II(e), which contain a sixth-order light-by-light-scattering subdiagarm internally, was handled by an automation procedure [13]. At least two independent codes for non-automated programs were written by different members of our collaboration in order to minimize human errors.

All integrals were numerically evaluated by VEGAS [39]. For some diagrams of the sets IV and V that contain cancellation of linear IR divergence within a diagram, we used the quadruple-precision arithmetics to avoid possible round-off errors of numerical calculations. The contribution of the tau-particle loop to a_e is negligible at present. Thus the sum of (6) and (9) gives effectively the total tenth-order QED contribution to a_e.

[1] D. Hanneke, S. Fogwell, and G. Gabrielse, Phys. Rev. Lett. **100**, 120801 (2008).

TABLE II. Summary of contributions to the tenth-order lepton $g-2$ from 32 gauge-invariant subsets. n_F is the number of vertex diagrams contributing to $A_1^{(10)}$. The numerical values of individual subsets were originally obtained in the references in the fifth column. The values $A_1^{(10)}$ of subsets I(d), I(f), II(a), II(b), and VI(c) in [10] are corrected as indicated by the asterisk. The corrected values are listed in this table.

set	n_F	$A_1^{(10)}$	$A_2^{(10)}(m_e/m_\mu)$	reference
I(a)	1	0.000 470 94 (6)	0.000 000 28 (1)	[10]
I(b)	9	0.007 010 8 (7)	0.000 001 88 (1)	[10]
I(c)	9	0.023 468 (2)	0.000 002 67 (1)	[10]
I(d)	6	0.003 801 7 (5)	0.000 005 46 (1)	[10]*
I(e)	30	0.010 296 (4)	0.000 001 60 (1)	[10]
I(f)	3	0.007 568 4 (20)	0.000 047 54 (1)	[10]*
I(g)	9	0.028 569 (6)	0.000 024 45 (1)	[12]
I(h)	30	0.001 696 (13)	−0.000 010 14 (3)	[12]
I(i)	105	0.017 47 (11)	0.000 001 67 (2)	[16]
I(j)	6	0.000 397 5 (18)	0.000 002 41 (6)	[11]
II(a)	24	−0.109 495 (23)	−0.000 737 69 (95)	[10]*
II(b)	108	−0.473 559 (84)	−0.000 645 62 (95)	[10]*
II(c)	36	−0.116 489 (32)	−0.000 380 25 (46)	[15]
II(d)	180	−0.243 00 (29)	−0.000 098 17 (41)	[15]
II(e)	180	−1.344 9 (10)	−0.000 465 0 (40)	[13]
II(f)	72	−2.433 6 (15)	−0.005 868 (39)	[10]
III(a)	300	2.127 33 (17)	0.007 511 (11)	[17]
III(b)	450	3.327 12 (45)	0.002 794 (1)	[17]
III(c)	390	4.921 (11)	0.003 70 (36)	[19]
IV	2072	−7.7296 (48)	−0.011 36 (7)	[18]
V	6354	10.09 (57)	0	Eq. (7)
VI(a)	36	1.041 32 (19)	0.006 152 (11)	[10]
VI(b)	54	1.346 99 (28)	0.001 778 9 (35)	[10]
VI(c)	144	−2.5289 (28)	−0.005 953 (59)	[10]*
VI(d)	492	1.8467 (70)	0.001 276 (76)	[14]
VI(e)	48	−0.4312 (7)	−0.000 750 (8)	[10]
VI(f)	180	0.7703 (22)	0.000 033 (7)	[10]
VI(g)	480	−1.5904 (63)	−0.000 497 (29)	[14]
VI(h)	630	0.1792 (39)	0.000 045 (9)	[14]
VI(i)	60	−0.0438 (12)	−0.000 326 (1)	[10]
VI(j)	54	−0.2288 (18)	−0.000 127 (13)	[10]
VI(k)	120	0.6802 (38)	0.000 015 6 (40)	[10]

[9] T. Aoyama, M. Hayakawa, T. Kinoshita, and M. Nio, Phys. Rev. Lett. 99, 110406 (2007); Phys. Rev. D 77, 053012 (2008).
[10] T. Kinoshita and M. Nio, Phys. Rev. D 73, 053007 (2006).
[11] T. Aoyama, M. Hayakawa, T. Kinoshita, M. Nio, and N. Watanabe, Phys. Rev. D 78, 053005 (2008).
[12] T. Aoyama, M. Hayakawa, T. Kinoshita, and M. Nio, Phys. Rev. D 78, 113006 (2008).
[13] T. Aoyama, K. Asano, M. Hayakawa, T. Kinoshita, M. Nio, and N. Watanabe, Phys. Rev. D 81, 053009 (2010).
[14] T. Aoyama, M. Hayakawa, T. Kinoshita, and M. Nio, Phys. Rev. D 82, 113004 (2010).
[15] T. Aoyama, M. Hayakawa, T. Kinoshita, and M. Nio, Phys. Rev. D 83, 053002 (2011).
[16] T. Aoyama, M. Hayakawa, T. Kinoshita, and M. Nio, Phys. Rev. D 83, 053003 (2011).
[17] T. Aoyama, M. Hayakawa, T. Kinoshita, and M. Nio, Phys. Rev. D 84, 053003 (2011).
[18] T. Aoyama, M. Hayakawa, T. Kinoshita, and M. Nio, Phys. Rev. D 85, 033007 (2012).
[19] T. Aoyama, M. Hayakawa, T. Kinoshita, and M. Nio, Phys. Rev. D 85, 093013 (2012).
[20] T. Aoyama, M. Hayakawa, T. Kinoshita, and M. Nio, in preparation.
[21] P. J. Mohr and B. N. Taylor, Rev. Mod. Phys. 72, 351 (2000).
[22] G. Gabrielse, D. Hanneke, T. Kinoshita, M. Nio, and B. Odom, Phys. Rev. Lett. 97, 030802 (2006); 99, 039902(E) (2007).
[23] H. H. Elend, Phys. Lett. 20, 682 (1966); 21, 720(E) (1966).
[24] M. A. Samuel and G.-w. Li, Phys. Rev. D 44, 3935 (1991).
[25] G. Li, R. Mendel, and M. A. Samuel, Phys. Rev. D 47, 1723 (1993).
[26] S. Laporta and E. Remiddi, Phys. Lett. B301, 440 (1993).
[27] S. Laporta, Nuovo Cim. A106, 675 (1993).
[28] M. Passera, Phys. Rev. D 75, 013002 (2007).
[29] M. Davier and A. Höcker, Phys. Lett. B435, 427 (1998).
[30] B. Krause, Phys. Lett. B390, 392 (1997).
[31] J. Prades, E. de Rafael, and A. Vainshtein, in Lepton Dipole Moments, edited by B. L. Roberts and W. J. Marciano (World Scientific, Singapore, 2009) pp. 303–319.
[32] K. Fujikawa, B. Lee, and A. Sanda, Phys. Rev. D 6, 2923 (1972).
[33] A. Czarnecki, B. Krause, and W. J. Marciano, Phys. Rev. Lett. 76, 3267 (1996).
[34] M. Knecht, S. Peris, M. Perrottet, and E. De Rafael, J. High Energy Phys. 11, 003 (2002).
[35] A. Czarnecki, W. J. Marciano, and A. Vainshtein, Phys. Rev. D 67, 073006 (2003).
[36] R. Bouchendira, P. Clade, S. Guellati-Khelifa, F. Nez, and F. Biraben, Phys. Rev. Lett. 106, 080801 (2011).
[37] M. Caffo, S. Turrini, and E. Remiddi, Nucl. Phys. B141, 302 (1978).
[38] T. Kinoshita and M. Nio, Phys. Rev. Lett. 90, 021803 (2003).
[39] G. P. Lepage, J. Comput. Phys. 27, 192 (1978).
[40] T. Aoyama, M. Hayakawa, T. Kinoshita, and M. Nio, Nucl. Phys. B740, 138 (2006); B796, 184 (2008).

[2] D. Hanneke, S. Fogwell Hoogerheide, and G. Gabrielse, Phys. Rev. A 83, 052122 (2011).
[3] P. J. Mohr, B. N. Taylor, and D. B. Newell, (2012), arXiv:1203.5425.
[4] J. S. Schwinger, Phys. Rev. 73, 416 (1948).
[5] A. Petermann, Helv. Phys. Acta 30, 407 (1957).
[6] C. M. Sommerfield, Ann. Phys. (N.Y.) 5, 26 (1958).
[7] S. Laporta and E. Remiddi, Phys. Lett. B379, 283 (1996).
[8] T. Kinoshita and M. Nio, Phys. Rev. D 73, 013003 (2006).